

## **Characterization of young and old adult brains: An EEG functional connectivity analysis**

Bahar Moezzi<sup>1,\*,+</sup>, Latha Madhuri Pratti\*, Brenton Hordacre<sup>2</sup>, Lynton Graetz<sup>3</sup>, Carolyn Berryman<sup>3</sup>, Louise M. Lavrencic<sup>1,4</sup>, Michael C. Ridding<sup>3</sup>, Hannah A. D. Keage<sup>1</sup>, Mark D. McDonnell<sup>5</sup>, Mitchell R. Goldsworthy<sup>3</sup>

<sup>1</sup> Cognitive Ageing and Impairment Neurosciences Laboratory, School of Psychology, Social Work and Social Policy, University of South Australia, Australia

<sup>2</sup> School of Health Sciences, University of South Australia, Australia

<sup>3</sup> Robinson Research Institute, Adelaide Medical School, University of Adelaide, Australia

<sup>4</sup> Neuroscience Research of Australia, Australia

<sup>5</sup> Computational Learning Systems Laboratory, School of Information Technology and Mathematical Sciences, University of South Australia, Australia

+ Corresponding author (Bahar Moezzi) email: [bahar.moezzi@mymail.unisa.edu.au](mailto:bahar.moezzi@mymail.unisa.edu.au)

\* Equal contributors

**Running title:** Classification of young and old brains

**Keywords:** functional connectivity, machine learning, ageing, resting-state, EEG

## Abstract

Brain connectivity studies have reported that functional networks change with older age. We aim to (1) investigate whether electroencephalography (EEG) data can be used to distinguish between individual functional networks of young and old adults; and (2) identify the functional connections that contribute to this classification. Two eyes-open resting-state EEG recording sessions with 64 electrodes for each of 22 younger adults (19-37 years) and 22 older adults (63-85 years) were conducted. For each session, imaginary coherence matrices in theta, alpha, beta and gamma bands were computed. A range of machine learning classification methods were utilized to distinguish younger and older adult brains. A support vector machine (SVM) classifier was 94% accurate in classifying the brains by age group. We report decreased functional connectivity with older age in theta, alpha and gamma bands, and increased connectivity with older age in beta band. Most connections involving frontal, temporal, and parietal electrodes, and approximately two-thirds of connections involving occipital electrodes, showed decreased connectivity with older age. Just over half of the connections involving central electrodes showed increased connectivity with older age. Functional connections showing decreased strength with older age had significantly longer electrode-to-electrode distance than those that increased with older age. Most of the connections used by the classifier to distinguish participants by age group belonged to the alpha band. Findings suggest a decrease in connectivity in key networks and frequency bands associated with attention and awareness, and an increase in connectivity of the sensorimotor functional networks with ageing during a resting state.

## 1. Introduction

Advanced age is associated with a progressive decline in cognition, particularly in the domains of attention, memory and executive function (Hedden & Gabrieli, 2004; Raz & Rodrigue, 2006). While there has been considerable research investigating the pathophysiological changes that characterize Alzheimer's disease and other age-related neurodegenerative disorders (Goedert & Spillantini, 2006; Y. Huang & Mucke, 2012), much less is known about the neural processes affecting cognition in normal, non-pathological ageing. A greater understanding of the basic neurophysiology of healthy human ageing may prove critical for devising novel therapeutic approaches for slowing or reversing age-related cognitive decline.

The long-range connectivity of resting-state brain networks decreases in healthy ageing (Esposito et al., 2008; Ferreira & Busatto, 2013; Hafkemeijer, van der Grond, & Rombouts, 2012; Koch et al., 2010; Meunier, Achard, Morcom, & Bullmore, 2009; Mevel, Chételat, Eustache, & Desgranges, 2011; Tomasi & Volkow, 2012). Using fMRI age-related decreases in resting-state functional connectivity have been observed in the default mode network (DMN) and the dorsal attention network (DAN) (Hafkemeijer et al., 2012; Mevel et al., 2011), both of which are heavily implicated in attention, memory and executive functions (van Den Heuvel & Hulshoff Pol, 2010). The DMN comprises a set of regions active at rest, including the medial prefrontal cortex, the inferior parietal lobule, the hippocampus and the posterior cingulate cortex/retrosplenial cortex/precuneus (Buckner, Andrews-Hanna, & Schacter, 2008). The DAN includes a set of brain regions comprising the prefrontal, anterior cingulate and posterior parietal cortices (Tomasi & Volkow, 2012).

It is suggested that age-related changes in the motor networks may be different from those in the DMN and the DAN. Using fMRI increased functional connectivity has been found in motor and subcortical networks in healthy ageing (Tomasi & Volkow, 2012). In a resting-state functional magnetic resonance imaging (fMRI) study of 913 healthy adults from the 1000 Functional Connectomes Project repository, Tomasi and Volkow (2012) observed that advancing age was associated with increased functional connectivity in the somatosensory and motor cortices, cerebellum and brainstem. However, other studies have reported reverse findings (Allen et al., 2011; Toussaint et al., 2011; T. Wu et al., 2007).

EEG is a non-invasive method of recording cortical activity through the scalp (Niedermeyer & da Silva, 2005). While the spatial resolution of EEG is limited compared to fMRI, its high temporal precision makes it possible to measure neural oscillations that occur in the millisecond time range due to synchronized rhythmical firing of populations of neurons (Niedermeyer & da Silva, 2005). This oscillatory activity is thought to play a key role in coordinating activity in large-scale brain networks, facilitating information flow between

distributed brain regions when oscillations are synchronized between regions (Siegel, Donner, & Engel, 2012). Neural oscillations are grouped into specific frequency bands, each reflecting neural activity within particular brain structures and under different brain states. For instance, theta band oscillations have been linked to hippocampal-dependent behaviours such as spatial navigation and learning (Araújo, Baffa, & Wakai, 2002; Kahana, Sekuler, Caplan, Kirschen, & Madsen, 1999), and are also increased in frontal and parietal brain regions during different types of working memory and attentional control tasks (Klimesch, Freunberger, Sauseng, & Gruber, 2008; Sauseng, Griesmayr, Freunberger, & Klimesch, 2010). Alpha band oscillations are dominant in occipital regions, particularly during relaxed wakefulness with eyes closed, and are also thought to play an important role in attention and working memory by gating sensory processing to protect information held online from sensory interference (Klimesch, Sauseng, & Hanslmayr, 2007). Beta band oscillations have been linked to sensorimotor network activity (Pfurtscheller, Stancak Jr, & Neuper, 1996; Roopun et al., 2006). Gamma band oscillations, on the other hand, have been associated with a range of sensory and cognitive processes (Başar, Başar-Eroglu, Karakaş, & Schürmann, 2001; Fries, 2009), although appear particularly affected by muscle and electrical noise (Pope, Fitzgibbon, Lewis, Whitham, & Willoughby, 2009; Whitham et al., 2007).

Functional connectivity can be estimated in specific frequency bands using EEG recordings (Sakkalis, 2011). Frequency specific changes in functional connectivity throughout the lifespan have been previously reported (Micheloyannis et al., 2009; Smit et al., 2012). Smit et al. (2012) investigated the change in the functional brain connectivity from ages 5 through 71 years using resting-state EEG. Smit et al. (2012) reported large increases in theta, alpha and beta functional connectivity from childhood to adolescence that continued at a slower pace into adulthood (peaking at 50 years) and decreases in theta, alpha and beta functional connectivity above 50 years. Micheloyannis et al. (2009) used resting-state and task (mathematical thinking) EEG from twenty children and twenty young adults and reported lower beta and gamma connectivity in both rest and during task in adults. Vysata et al. (2014) used resting-state EEG in a group of 17,722 healthy professional drivers with a mean age of 43.2 years (SD = 11.2 years) and reported average functional connectivity over the whole scalp increased with older age in the beta band and decreased with older age in theta and alpha bands. However, it is still unknown how frequency-specific functional connections change with older age

Machine learning classifiers (Pereira, Mitchell, & Botvinick, 2009) provide a powerful approach to investigate age-related differences in functional networks. One of the commonly used machine learning classifiers is support vector machine (SVM). A crucial aspect of SVM is that it identifies the features that drive classifier performance. An SVM algorithm trained on

a training dataset can generate feature weights corresponding to the relative contribution of an individual feature to successful differentiation of the two groups. Following this, the classifier can be applied to a separate testing dataset to assess the accuracy of the classifier in differentiating the two groups. SVM classifiers have been used to classify individual brains by chronological age using resting-state fMRI connectivity data. Dosenbach et al. (2010) used data from 238 fMRI scans of participants aged 7 to 30 years old. They classified children and adult brains with 91% accuracy, which was replicated as 92% and 93% accuracy with two other datasets comprising of 195 and 186 scans. Meier et al. (2012) used three scans from 26 younger adults (18-35 years old) and 26 older adults (55-85 years old) and were able to classify younger and older adult brains with 84% accuracy. They showed that the majority of the functional connections that distinguished older and younger adults came from regions belonging to the sensorimotor and cingulo-opercular functional networks. They reported a decrease in long-range functional connectivity and an increase in short-range functional connectivity with older age. Machine learning has been successfully applied to resting-state EEG data in the classification of typically developing children from a group of infants at high risk for autism spectrum disorder (Kousarrizi, Ghanbari, Gharaviri, Teshnehlab, & Aliyari, 2009) and in the classification of alcoholics and non-alcoholics (Bosl, Tierney, Tager-Flusberg, & Nelson, 2011). Investigating EEG functional connectivity characteristics of healthy ageing will provide further understanding of the physiological processes that mediate changes in functional connectivity as humans age.

We aim at uncovering whether an individual resting EEG session can be used to distinguish young and old brains and most importantly, the identity of the functional connections that contribute to such classification. We hypothesized that long-range functional connectivity of theta and alpha band oscillations, particularly in frontal, parietal and occipital regions, would be decreased with older age.

## **2. Materials and Methods**

### **2.1. Procedure**

Resting-state EEG data from 22 younger adults aged 19 to 37 years (mean 24.3 years, SD 6.1 years, 9 male, 21 self-reported right-handed) and 22 older adults aged 63 to 85 years (mean 71 years, SD 6 years, 9 male, 22 right-handed according to the Flinders Handedness Survey (Nicholls, Thomas, Loetscher, and Grimshaw (2013)) were recorded. In line with Meier et al. (2012) we used more than one recording session from each participant. Our dataset consists of two separate resting-state recording sessions for each participant, recorded at least 7 days apart. The EEG recordings were baseline measurements in pre-intervention or sham conditions embedded in larger studies on the effects of transcranial magnetic stimulation and/or Noxious stimulation on brain dynamics. The EEG data for

younger adults is published elsewhere in the context of a graph theoretical analysis (Moezzi, Hordacre, Berryman, Ridding, & Goldsworthy, 2018). Participants gave written informed consent in accordance with the World Medical Association Declaration of Helsinki to participate in this study. Ethical approval was provided by the University of Adelaide Human Research Ethics Committee and University of South Australia's Human Research Ethics Committee.

## **2.2. EEG acquisition and pre-processing**

We acquired three minutes of continuous resting-state EEG data (eyes open) using an ASA-lab EEG system (ANT Neuro, Enschede, Netherlands) or a TMSi EEG system (Twente Medical Systems International B.V, Oldenzaal, The Netherlands) using a Waveguard™ original cap with 64 sintered Ag-AgCl electrodes in standard 10-10 positions. During recording, participants were instructed to view a fixation point, remain still, quiet and relaxed to avoid blinking too much. Each participant's two sessions were performed using the same EEG system. Signals were sampled at 2048 Hz, amplified 20 times, filtered (high pass, DC; low pass 553 Hz) and referenced to the average of all electrodes. Impedance was kept below 5 k $\Omega$  and the recorded data were stored on a computer for offline analysis.

EEG data were exported to MATLAB 9.0 (MathWorks, Inc., Natick, MA) for pre-processing and analysis. The EEG signals were segmented into epochs of 1 second. The baseline means were removed from the EEG dataset. Channels Fp1, Fpz, Fp2, M1, M2, AF7 and AF8 and channels that were disconnected during recording or dominated by exogenous artefact noise were removed. The data were filtered using a hamming windowed sinc finite impulse response filter (1-45 Hz). We excluded epochs contaminated by excessive deflection identified by a threshold for the maximum allowed amplitude for the EEG signals >100  $\mu$ V (7% of epochs were excluded). Fast ICA artefact correction was implemented to correct for non-physiological artefacts (e.g. eye blinks and scalp muscle activity) (Delorme & Makeig, 2004). Missing channels were interpolated using super-fast spherical interpolation.

## **2.3. Power**

We used the power spectra to set the range of the theta, alpha, beta and gamma frequency bands separately for younger and older adults. We computed power-spectra by performing time-frequency analysis on EEG time series over multiple trials using the multitaper method based on Hanning tapers. The analysis windows were centred in each trial at 0.01 s intervals with three cycles per time window. In line with (Haegens, Cousijn, Wallis, Harrison, & Nobre, 2014; Moretti et al., 2011), our alpha frequency was defined as the biggest local maximum within the extended range (5–14 Hz). The theta/alpha transition frequency (TF) was computed as the minimum power in the alpha frequency range. Theta band was defined

from 4 Hz to TF. The gamma frequency was defined as the highest peak with frequency above 30 Hz (Herrmann, Lenz, Junge, Busch, & Maess, 2004) and up to 45 Hz (Hordacre, Moezzi, & Ridding, 2018). The beta band was defined as the frequencies between the higher endpoint of the alpha band and 30 Hz (Henelius, Korpela, & Huutilainen, 2011). We utilized FieldTrip which is a MATLAB software toolbox for EEG and MEG analysis to compute power (Oostenveld & Praamstra, 2001).

#### 2.4. Functional connectivity

We constructed the functional connectivity matrices for each participant using imaginary coherence in theta, alpha, beta and gamma frequency bands. The  $l$ -th segment of the  $i$ -th time course is denoted by  $x_{i,l}$  and its Fourier transform by  $X_{i,l}$ . The cross-spectral matrix is defined as

$$S_{i,j} = \frac{1}{N} \sum_{l=1}^K X_{i,l}^* X_{j,l} \quad (1)$$

where  $(\cdot)^*$  denotes complex conjugation and  $N$  denotes the total number of segments. The coherency between the  $i$ -th and  $j$ -th times series is defined as

$$C_{i,j} = \frac{S_{i,j}}{\sqrt{S_{i,i}S_{j,j}}} \quad (2)$$

We computed the absolute value of imaginary coherence between each two EEG electrodes  $m$  and  $n$  as

$$J_{p,q} = |\zeta(C_{i_m,j_n})| \quad (3)$$

where  $\zeta(\cdot)$  denotes the imaginary part. Finally, matrix  $J$  was divided by its standard deviation using the Jackknife method to generate a connectivity matrix. To compute functional connectivity, we utilized the FieldTrip software package (Oostenveld & Praamstra, 2001).

#### 2.5 Classification

Soft-margin SVM classification was performed using Scikit-Learn, a machine learning toolbox implemented in Python (Pedregosa et al., 2011). Local Outlier Factor and Isolation Forest algorithms were used to identify outliers (Breunig, Kriegel, Ng, & Sander, 2000; Liu, Ting, & Zhou, 2008). In line with previous literature, we mapped the data in higher-dimension using a radial basis function (RBF) as the underlying kernel and discriminated functional connectivity data as belonging to the younger or older adult group using a linear decision function (Meier et al., 2012). A leave-one-out cross-validation (LOOCV) procedure was performed to (1) identify the most significant features, (2) tune the hyper-parameters (C-regularization factor and gamma-kernel coefficient) of SVM and (3) determine the accuracy

of the classifier. For each iteration of LOOCV, both sessions of a participant were removed, and the top 300 features (functional connections) were selected using two-sample t-tests on the training set and ranked according to their absolute t-statistics. We used the resulting t-scores as our feature weights. We kept 300 features because this was the approximate number of features that remained significant following False Discovery Rate correction. After selecting the top features, a nested LOOCV was performed to train the classifier and tune the hyperparameters. In the outer LOOCV loop, both the sessions of a participant were set aside for validating the classifier. The sessions of the remaining participants were used in the inner LOOCV loop to tune the hyperparameters of the classifier. Once the classifier is trained, the left-out sessions were separately classified as belonging to the younger or older adult group. The total accuracy of the classifier was determined by the percent of correctly classified sessions across all iterations. Receiver operating characteristics (ROC) curve was considered to calculate the area under curve score for a dataset having balanced classes (Fawcett, 2006). ROC takes into consideration the value of the threshold that identifies which class the session belongs to. A perfect classifier has a score of 1 whereas a classifier operating at random has a score of 0.5. For each group, young and old, the precision of the classifier was determined as the number of true positives divided by the sum of true positives and false positives. The recall of the classifier was determined by the number of true positives divided by the sum of true positives and false negatives.

Due to equal number of older and younger adults, the chance performance of the classifier generates an accuracy of 50%. In line with previous literature, we considered each iteration of the LOOCV as a Bernoulli trial with success probability of 0.5 (Pereira et al., 2009). By comparing the number of true positives to the number of sessions to be classified we also determined the probability of the accuracy occurring by chance.

In addition to SVM, we performed classification using alternative methods. Once the most significant features were identified, the LOOCV procedure was performed to tune the hyperparameters and determine the accuracy of each of the following methods: K-nearest neighbours (Cover & Hart, 1967) was performed by tuning the number of nearest neighbours, least squares linear classifier (Bishop, 2006), SVM classifier with linear kernel by tuning the regularization factor (C), and extreme learning machine (ELM) (Akusok, Bjork, Miche, & Lendasse, 2015; G.-B. Huang, Zhu, & Siew, 2004) with linear, RBF and sigmoid kernels by tuning the number of neurons to be added to the network.

## **2.6. Brain regions**

We categorized electrodes into groups approximating frontal, central, parietal, temporal, and occipital brain regions based on an EEG study by Kamarajan et al. (2015) – see Figure 1. To compute the contribution of each region to the SVM classification, if a feature consisted of



two electrodes from different brain regions, then half of the feature weight was assigned to each brain region. If both electrodes of a feature were from the same region, then the full feature weight was assigned to that region. The percentage contribution of each region was then normalized to account for differences in the total number of electrodes included in each region.

## **2.7. Electrode-to-electrode distance**

We characterized consensus features by the Euclidian distance between electrode pairs to investigate patterns of age-related differences. The 3-D electrode template we used was a standard 10-5 template constructed by Oostenveld and Praamstra (2001) electrode positions represented in millimetre in the Montreal Neurological Institute (MNI) coordinate system.

## **2.8. Statistical analysis**

We compared the connections that decreased with older age to those that increased with older age based on electrode-to-electrode Euclidian distance using Mann-Whitney *U*-test. *P*-values < 0.05 were considered statistically significant.

## **3 Results**

### **3.1. Power**

We plotted the power spectra for younger and older adults for theta, alpha, beta and gamma bands (see Figure 2). For older adults, frequency ranges of 4-6 Hz and 7-13 Hz were selected for theta and alpha bands, respectively, whereas for younger adults, 4-7 Hz and 8-13 Hz were used. We set beta band to 14-30 Hz and gamma band to 31-45 Hz for both younger and older adults. While we used the power spectra to set the frequency bands we continue with analysing on functional connectivity data. Our main goal is to identify the distinguishing age-related differences in functional connectivity.

### **3.2. Outliers**

Of the 88 separate EEG recording sessions, Local Outlier Factor algorithm identified seven outliers, four of which belonged to the younger adult group and three to the older adult group. These same outliers were detected using Isolation Forest algorithm and therefore were removed from the dataset prior to SVM classification. To maintain equal numbers of sessions for both younger and older groups, we also randomly selected a session from the older adult group and removed it from the dataset.

### **3.3. Classifier performance**

The classifier successfully classified younger adults from older adults with an accuracy of 94%. The 94% accuracy of the classifier was significantly higher than the accuracy by

chance performance of the classifier ( $p < 10^{-8}$ ). Five recording sessions belonging to the older adult group were misclassified with one older adult having both sessions misclassified.

The accuracy achieved by the SVM (linear kernel), k-nearest neighbours, ELM (linear kernel), ELM (RBF kernel), ELM (sigmoid kernel) and least squares linear classifier was below 84%. The accuracy, area under ROC curve, precision and recall values for all the methods are summarized in Table 1. The SVM classifier with RBF kernel has the highest accuracy, area under ROC curve, precision and recall among all the methods tested.

### **3.4. Features**

The features were analysed to uncover the patterns of functional connectivity changes that contributed to the SVM classification. From approximately 300 features obtained from each iteration of LOOCV, 162 features were identified to be common among all iterations (consensus features) – see Supplementary material Table 2. Eighty three percent of total consensus feature weights came from pairs of electrodes that showed lower functional connectivity in older adults than younger adults.

#### **3.4.1 Frequency bands**

We further analysed the consensus features belonging to theta, alpha, beta and gamma frequency bands. The frequency band with the greatest amount of consensus feature weight associated with it was the alpha band (112 of 162 consensus features), followed by beta (28 features), theta (17 features), and gamma (5 features) (Figure 3). The consensus features belonging to theta, alpha and gamma bands had positive weights showing significantly higher functional connectivity in younger adults than in older adults. Consensus features of the beta band had negative weights showing significantly higher functional connectivity in older adults than younger adults.

#### **3.4.2. Brain regions**

Electrodes were grouped as approximating five brain regions (temporal, frontal, occipital, parietal, central). The single electrode with the greatest amount of consensus feature weight associated with it was TP7 (temporal) followed by T7 (temporal), Pz (parietal), P2 (parietal) and POz (occipital). As seen in Figure 4, the large majority of features involving frontal, temporal, and parietal electrodes, and approximately two-thirds of features involving occipital electrodes, showed decreased connectivity with older age. Conversely, slightly more than half of the features involving central electrodes showed increased connectivity with older age.

### 3.4.3. Distance

We compared the connections that decreased with older age to those that increased with older age based on electrode-to-electrode Euclidian distance. We observed that consensus features showing decreased functional connectivity with older age were longer than those that showed increased connectivity with older age ( $U = 1289$ ,  $Z = -2.6$ ,  $p = 0.009$ ; decrease: median = 140.9 mm, range = 29.4-185.4 mm; increase: median = 120.8 mm, range = 36.8-156.0 mm) – see Figure 5.

## 4. Discussion

The greatest contribution to the classification of young from old brains came from a decrease in functional connectivity of electrodes approximating the frontal, parietal and temporal areas in older compared to young adults, particularly in alpha band. We also observed an age-related increase in functional connectivity of electrodes approximating the motor regions in the beta band. Our findings suggest a decrease in connectivity in key networks and frequency bands associated with attention and an increase in the networks and frequency band associated with motor control with advanced ageing

Ageing is characterized by alterations in functional brain networks (Ferreira & Busatto, 2013; Hedden & Gabrieli, 2004; Raz & Rodrigue, 2006; Rossini, Rossi, Babiloni, & Polich, 2007). Resting-state functional connectivity has shown to commonly decrease in healthy aging (for a review see Ferreira and Busatto (2013)). Most commonly, using fMRI decreases in frontal and parietal areas with older ageing have been observed (Hafkemeijer et al., 2012; Mevel et al., 2011). In line with this, we found that the most influential connections for classifier performance were those showing decreased connectivity with older age. This was largely due to connections involving frontal, temporal, parietal, and (to a lesser extent) occipital electrodes, with the greatest contribution coming from decreased connectivity in the alpha frequency band.

The decreased alpha band connectivity of frontal and parietal areas in older relative to younger adults may reflect changes in attentional and arousal levels with advanced ageing (Mathewson et al., 2012), with theta and alpha band oscillations suggested to reflect attentional load and arousal level (Klimesch, 2012; Klimesch, Doppelmayr, Russegger, Pachinger, & Schwaiger, 1998; Mathewson et al., 2012). Using EEG and MEG recordings, decreased alpha connectivity of frontal, parietal and temporal regions have been observed in pathological mild cognitive impairment and dementia (Babiloni et al., 2018; Babiloni et al., 2006; Babiloni et al., 2004; Bosboom, Stoffers, Wolters, Stam, & Berendse, 2009). A frontoparietal network is often engaged during tasks requiring attention (Bonnelle et al.,

2011; Coull, Frackowiak, & Frith, 1998) so a decrease in frontoparietal connectivity is likely to reflect impaired attention.

Whereas consensus features for alpha, theta, and gamma bands all showed decreased functional connectivity with older age, features for beta showed increased connectivity in older relative to younger adults, accounting for 17% of the total feature weight. Neural oscillations in the beta frequency band have been strongly linked to sensorimotor network activity (Pfurtscheller et al., 1996; Roopun et al., 2006), with resting-state beta connectivity associated with motor cortex function and plasticity in healthy subjects (Hordacre et al., 2017; J. Wu, Srinivasan, Kaur, & Cramer, 2014) and after stroke (J. Wu et al., 2015). The beta band features in this study mostly involved central electrodes overlying sensorimotor networks. FMRI studies have shown age-related increases in functional connectivity of sensorimotor networks both during task performance (Heitger et al., 2013) and at rest (Langan et al., 2010; Meier et al., 2012; Mowinckel, Espeseth, & Westlye, 2012; Solesio-Jofre et al., 2014; Tomasi & Volkow, 2012), reflecting a loss of functional segregation among sensorimotor areas that is related to poorer performance on motor coordination tasks (Solesio-Jofre et al., 2014). While less is known about the role of resting-state beta rhythms in ageing, there is some evidence that advanced age is associated with increases in both resting-state beta power and beta de-synchronization during movement, possibly reflecting changes in the balance between GABAergic inhibition and glutamatergic excitation in the aged motor cortex (Rossiter, Davis, Clark, Boudrias, & Ward, 2014). Our results showing increased beta band functional connectivity and decreased theta and alpha band functional connectivity with older age are in agreement with previous research (Vysata et al., 2014). While age differences in excitatory-inhibitory balance might have contributed to age-related increases in beta band functional connectivity to classifier performance in the present study (Rossiter et al., 2014), additional research is needed to explore this further.

We observed that consensus features showing decreased functional connectivity with older age were significantly longer than those that showed increased connectivity with older age. This is in agreement with the findings of Meier et al. (2012), who reported a decrease in long-range functional connectivity and an increase in short-range functional connectivity with older age. While the physiological significance of distances separating surface electrode pairs should be interpreted with caution, these data are consistent with the notion that long-range connections, particularly between anterior and posterior brain regions, are more affected than short-range connections in normal and pathological ageing (Sala-Llonch et al., 2014; Tomasi & Volkow, 2012).

There are several limitations to this study. First, we acknowledge that EEG suffers from poor spatial resolution and signals that are recorded at the surface level can be affected by

volume conduction (Bastos & Schoffelen, 2016). We have tried to mitigate this effect by using a conservative measure of functional connectivity (i.e. imaginary coherence). However, this may not thoroughly remove the effects of volume conduction and caution is needed when suggesting generators of the neural signal recorded with EEG surface electrodes. Second, the use of SVM requires several user decisions. For example, for estimating parameters we had to choose an appropriate kernel and its parameters. Because the data was not linearly separable, we chose a radial RBF kernel which projects the data to infinite dimensions and linearly separates both the groups (Meier et al., 2012). The parameters for the kernel are estimated using the nested leave one out cross-validation procedure. Finally, as mentioned above, it is important to note that using the Euclidian distance between electrodes does not reflect the distance of physical connections.

In summary, we show that an individual resting-state EEG recording can be used to classify younger adult brains from older adult brains with high accuracy, enabling greater understanding of functional connectivity as a mechanism mediating changes in human behaviour with ageing. Our study supports the literature that suggest functional connectivity of frontal, parietal and temporal regions decreases, and connectivity of motor areas increases with older age. These findings also emphasize the role of alpha frequency band connectivity in characterizing advanced ageing.

## **Acknowledgements**

MRG is supported by a NHMRC-ARC Dementia Research Development Fellowship (1102272). HADK is supported by a NHMRC Boosting Dementia Research Leadership Fellowship (GNT1135676). BH funded by a NHMRC fellowship (1125054). CB is funded by a NHMRC fellowship (1127155). BM would like to thank Luke Hallam for helpful discussions. We would like to thank all of the participants that made this work possible.

## References

- Akusok, A., Bjork, K.-M., Miche, Y., & Lendasse, A. (2015). High-Performance Extreme Learning Machines: A Complete Toolbox for Big Data Applications. *Access, IEEE*, 3, 1011-1025. doi:10.1109/access.2015.2450498
- Allen, E. A., Erhardt, E. B., Damaraju, E., Gruner, W., Segall, J. M., Silva, R. F., . . . Calhoun, V. D. (2011). A Baseline for the Multivariate Comparison of Resting-State Networks. *Frontiers in Systems Neuroscience*, 5(2011). doi:10.3389/fnsys.2011.00002
- Araújo, D. B. d., Baffa, O., & Wakai, R. T. (2002). Theta oscillations and human navigation: a magnetoencephalography study. *Journal of Cognitive Neuroscience*, 14(1), 70-78. doi:10.1162/089892902317205339
- Babiloni, C., Del Percio, C., Lizio, R., Noce, G., Lopez, S., Soricelli, A., . . . Stocchi, F. (2018). Functional cortical source connectivity of resting state electroencephalographic alpha rhythms shows similar abnormalities in patients with mild cognitive impairment due to Alzheimer's and Parkinson's diseases. *Clinical Neurophysiology*, 129(4), 766-782. doi:10.1016/j.clinph.2018.01.009
- Babiloni, C., Ferri, R., Binetti, G., Cassarino, A., Forno, G. D., Ercolani, M., . . . Rossini, P. M. (2006). Fronto-parietal coupling of brain rhythms in mild cognitive impairment: A multicentric EEG study. *Brain Research Bulletin*, 69(1), 63-73. doi:10.1016/j.brainresbull.2005.10.013
- Babiloni, C., Ferri, R., Moretti, D. V., Strambi, A., Binetti, G., Ferreri, F., . . . Rossini, P. M. (2004). Abnormal fronto-parietal coupling of brain rhythms in mild Alzheimer's disease: a multicentric EEG study. *European Journal of Neuroscience*, 19(9), 2583-2590. doi:10.1111/j.0953-816X.2004.03333.x
- Başar, E., Başar-Eroglu, C., Karakaş, S., & Schürmann, M. (2001). Gamma, alpha, delta, and theta oscillations govern cognitive processes. *International Journal of Psychophysiology*, 39(2), 241-248. doi:10.1016/s0167-8760(00)00145-8
- Bastos, A. M., & Schoffelen, J.-M. (2016). A Tutorial Review of Functional Connectivity Analysis Methods and Their Interpretational Pitfalls.(Report)(Author abstract). *Frontiers in Systems Neuroscience*, 9(2016). doi:10.3389/fnsys.2015.00175
- Bishop, C. M. (2006). *Pattern recognition and machine learning*. New York: Springer.
- Bonnelle, V., Leech, R., Kinnunen, K. M., Ham, T. E., Beckmann, C. F., De Boissezon, X., . . . Sharp, D. J. (2011). Default mode network connectivity predicts sustained attention

- deficits after traumatic brain injury. *Journal of Neuroscience*, 31(38), 13442-13451.  
doi:10.1523/JNEUROSCI.1163-11.2011
- Bosboom, J., Stoffers, D., Wolters, E. C., Stam, C. J., & Berendse, H. W. (2009). MEG resting state functional connectivity in Parkinson's disease related dementia. *Journal of Neural Transmission*, 116(2), 193-202. doi:10.1007/s00702-008-0132-6
- Bosl, W., Tierney, A., Tager-Flusberg, H., & Nelson, C. A. (2011). EEG complexity as a biomarker for autism spectrum disorder risk. *BMC Medicine*, 9(1). doi:10.1186/1741-7015-9-18
- Breunig, M., Kriegel, H., Ng, R., & Sander, J. (2000). LOF: Identifying density-based local outliers. *Sigmod Record*, 29(2), 93-104. doi:10.1145/335191.335388
- Buckner, R. L., Andrews-Hanna, J. R., & Schacter, D. L. (2008). The brain's default network: anatomy, function, and relevance to disease. *Annals of the New York Academy of Sciences*, 1124(1), 1. doi:10.1196/annals.1440.011
- Coull, J. T., Frackowiak, R. S., & Frith, C. D. (1998). Monitoring for target objects: activation of right frontal and parietal cortices with increasing time on task. *Neuropsychologia*, 36(12), 1325-1334. doi:10.1016/S0028-3932(98)00035-9
- Cover, T., & Hart, P. (1967). Nearest neighbor pattern classification. *Information Theory, IEEE Transactions on*, 13(1), 21-27. doi:10.1109/tit.1967.1053964
- Delorme, A., & Makeig, S. (2004). EEGLAB: an open source toolbox for analysis of single-trial EEG dynamics including independent component analysis. *Journal of neuroscience methods*, 134(1), 9-21. doi:10.1016/j.jneumeth.2003.10.009
- Dosenbach, N., Nardos, B., Cohen, A., Fair, D., Power, J., Church, J., . . . Schlaggar, B. (2010). Prediction of Individual Brain Maturity Using fMRI. *Science*, 329(5997), 1358-1361. doi:10.1126/science.1194144
- Esposito, F., Aragri, A., Pesaresi, I., Cirillo, S., Tedeschi, G., Marciano, E., . . . Di Salle, F. (2008). Independent component model of the default-mode brain function: combining individual-level and population-level analyses in resting-state fMRI. *Magnetic Resonance Imaging*, 26(7), 905-913. doi:10.1016/j.mri.2008.01.045
- Fawcett, T. (2006). An introduction to ROC analysis. *Pattern Recognition Letters*, 27(8), 861-874. doi:10.1016/j.patrec.2005.10.010
- Ferreira, L. K., & Busatto, G. F. (2013). Resting-state functional connectivity in normal brain aging. *Neuroscience Biobehavioral Reviews*, 37(3), 384-400.  
doi:10.1016/j.neubiorev.2013.01.017



- Fries, P. (2009). Neuronal gamma-band synchronization as a fundamental process in cortical computation. *Annual Review of Neuroscience*, 32, 209-224.  
doi:10.1146/annurev.neuro.051508.135603
- Goedert, M., & Spillantini, M. G. (2006). A century of Alzheimer's disease. *Science*, 314(5800), 777-781. doi:10.1126/science.1132814
- Haegens, S., Cousijn, H., Wallis, G., Harrison, P. J., & Nobre, A. C. (2014). Inter-and intra-individual variability in alpha peak frequency. *NeuroImage*, 92, 46-55.  
doi:10.1016/j.neuroimage.2014.01.049
- Hafkemeijer, A., van der Grond, J., & Rombouts, S. A. (2012). Imaging the default mode network in aging and dementia. *Biochimica et Biophysica Acta -Molecular Basis of Disease*, 1822(3), 431-441. doi:10.1016/j.bbadis.2011.07.008
- Hedden, T., & Gabrieli, J. D. (2004). Insights into the ageing mind: a view from cognitive neuroscience. *Nature Reviews Neuroscience*, 5(2), 87. doi:10.1038/nrn1323
- Heitger, M. H., Goble, D. J., Dhollander, T., Dupont, P., Caeyenberghs, K., Leemans, A., . . . Swinnen, S. P. (2013). Bimanual motor coordination in older adults is associated with increased functional brain connectivity—a graph-theoretical analysis. *PloS One*, 8(4), e62133. doi:10.1371/journal.pone.0062133
- Henelius, A., Korpela, J., & Huotilainen, M. (2011). *Individualising EEG frequency bands for sleep deprivation studies*. Paper presented at the Engineering in Medicine and Biology Society, EMBC, 2011 Annual International Conference of the IEEE.
- Herrmann, C. S., Lenz, D., Junge, S., Busch, N. A., & Maess, B. (2004). Memory-matches evoke human gamma-responses. *BMC Neuroscience*, 5(1), 13. doi:10.1186/1471-2202-5-13
- Hordacre, B., Moezzi, B., Goldsworthy, M. R., Rogasch, N. C., Graetz, L. J., & Ridding, M. C. (2017). Resting state functional connectivity measures correlate with the response to anodal transcranial direct current stimulation. *European Journal of Neuroscience*, 45(6), 837-845. doi:10.1111/ejn.13508
- Hordacre, B., Moezzi, B., & Ridding, M. C. (2018). Neuroplasticity and network connectivity of the motor cortex following stroke: A transcranial direct current stimulation study. *Human Brain Mapping*. doi:10.1002/hbm.24079
- Huang, G.-B., Zhu, Q.-Y., & Siew, C.-K. (2004). *Extreme learning machine: a new learning scheme of feedforward neural networks*. Paper presented at the Neural Networks, 2004. Proceedings. 2004 IEEE International Joint Conference on.

- Huang, Y., & Mucke, L. (2012). Alzheimer mechanisms and therapeutic strategies. *Cell*, 148(6), 1204-1222. doi:10.1016/j.cell.2012.02.040
- Kahana, M. J., Sekuler, R., Caplan, J. B., Kirschen, M., & Madsen, J. R. (1999). Human theta oscillations exhibit task dependence during virtual maze navigation. *Nature*, 399(6738), 781. doi:10.1038/21645
- Kamarajan, C., Pandey, A. K., Chorlian, D. B., Manz, N., Stimus, A. T., Anokhin, A. P., . . . Bucholz, K. K. (2015). Deficient event-related theta oscillations in individuals at risk for alcoholism: a study of reward processing and impulsivity features. *PloS One*, 10(11), e0142659. doi:10.1371/journal.pone.0142659
- Klimesch, W. (2012). Alpha-band oscillations, attention, and controlled access to stored information. *Trends in cognitive sciences*, 16(12), 606-617. doi:10.1016/j.tics.2012.10.007
- Klimesch, W., Doppelmayr, M., Russegger, H., Pachinger, T., & Schwaiger, J. (1998). Induced alpha band power changes in the human EEG and attention. *Neuroscience letters*, 244(2), 73-76. doi:10.1016/S0304-3940(98)00122-0
- Klimesch, W., Freunberger, R., Sauseng, P., & Gruber, W. (2008). A short review of slow phase synchronization and memory: evidence for control processes in different memory systems? *Brain Research*, 1235, 31-44. doi:10.1016/j.brainres.2008.06.049
- Klimesch, W., Sauseng, P., & Hanslmayr, S. (2007). EEG alpha oscillations: the inhibition-timing hypothesis. *Brain Research Reviews*, 53(1), 63-88. doi:10.1016/j.brainresrev.2006.06.003
- Koch, W., Teipel, S., Mueller, S., Buerger, K., Bokde, A. L., Hampel, H., . . . Meindl, T. (2010). Effects of aging on default mode network activity in resting state fMRI: does the method of analysis matter? *NeuroImage*, 51(1), 280-287. doi:10.1016/j.neuroimage.2009.12.008
- Kousarrizi, M. R. N., Ghanbari, A. A., Gharaviri, A., Teshnehlab, M., & Aliyari, M. (2009). *Classification of alcoholics and non-alcoholics via EEG using SVM and neural networks*. Paper presented at the Bioinformatics and Biomedical Engineering, 2009. ICBBE 2009. 3rd International Conference on.
- Langan, J., Peltier, S., Bo, J., Fling, B. W., Welsh, R. C., & Seidler, R. D. (2010). Functional implications of age differences in motor system connectivity. *Frontiers in Systems Neuroscience*, 4, 17. doi:10.3389/fnsys.2010.00017
- Liu, F. T., Ting, K. M., & Zhou, Z.-H. (2008). *Isolation forest*. Paper presented at the 2008 Eighth IEEE International Conference on Data Mining.

- Mathewson, K. E., Prudhomme, C., Fabiani, M., Beck, D. M., Lleras, A., & Gratton, G. (2012). Making waves in the stream of consciousness: entraining oscillations in EEG alpha and fluctuations in visual awareness with rhythmic visual stimulation. *Journal of Cognitive Neuroscience*, *24*(12), 2321-2333. doi:10.1162/jocn\_a\_00288
- Meier, T. B., Desphande, A. S., Vergun, S., Nair, V. A., Song, J., Biswal, B. B., . . . Prabhakaran, V. (2012). Support vector machine classification and characterization of age-related reorganization of functional brain networks. *NeuroImage*, *60*(1), 601-613. doi:10.1016/j.neuroimage.2011.12.052
- Meunier, D., Achard, S., Morcom, A., & Bullmore, E. (2009). Age-related changes in modular organization of human brain functional networks. *NeuroImage*, *44*(3), 715-723. doi:10.1016/j.neuroimage.2008.09.062
- Mevel, K., Chételat, G., Eustache, F., & Desgranges, B. (2011). The default mode network in healthy aging and Alzheimer's disease. *International Journal of Alzheimer's Disease*, *2011*. doi:10.4061/2011/535816
- Micheloyannis, S., Vourkas, M., Tsirka, V., Karakonstantaki, E., Kanatsouli, K., & Stam, C. J. (2009). The influence of ageing on complex brain networks: a graph theoretical analysis. *Human Brain Mapping*, *30*(1), 200-208. doi:10.1002/hbm.20492
- Moezzi, B., Hordacre, B., Berryman, C., Ridding, M. C., & Goldsworthy, M. R. (2018). Test-retest reliability of functional brain network characteristics using resting-state EEG and graph theory. *bioRxiv*, 385302. doi:10.1101/385302
- Moretti, D., Frisoni, G. B., Fracassi, C., Pievani, M., Geroldi, C., Binetti, G., . . . Zanetti, O. (2011). MCI patients' EEGs show group differences between those who progress and those who do not progress to AD. *Neurobiology of Aging*, *32*(4), 563-571. doi:10.1016/j.neurobiolaging.2009.04.003
- Mowinckel, A. M., Espeseth, T., & Westlye, L. T. (2012). Network-specific effects of age and in-scanner subject motion: a resting-state fMRI study of 238 healthy adults. *NeuroImage*, *63*(3), 1364-1373. doi:10.1016/j.neuroimage.2012.08.004
- Nicholls, M. E., Thomas, N. A., Loetscher, T., & Grimshaw, G. M. (2013). The Flinders Handedness survey (FLANDERS): A brief measure of skilled hand preference. *Cortex*, *49*(10), 2914-2926. doi:10.1016/j.cortex.2013.02.002
- Niedermeyer, E., & da Silva, L. F. (2005). *Electroencephalography: basic principles, clinical applications, and related fields*: Lippincott Williams & Wilkins.

- Oostenveld, R., & Praamstra, P. (2001). The five percent electrode system for high-resolution EEG and ERP measurements. *Clinical neurophysiology*, 112(4), 713-719. doi:10.1016/S1388-2457(00)00527-7
- Pedregosa, F., Varoquaux, G., Gramfort, A., Michel, V., Thirion, B., Grisel, O., . . . Dubourg, V. (2011). Scikit-learn: Machine learning in Python. *Journal of Machine Learning Research*, 12(Oct), 2825-2830.
- Pereira, F., Mitchell, T., & Botvinick, M. (2009). Machine learning classifiers and fMRI: a tutorial overview. *NeuroImage*, 45(1), S199-S209. doi:10.1016/j.neuroimage.2008.11.007
- Pfurtscheller, G., Stancak Jr, A., & Neuper, C. (1996). Post-movement beta synchronization. A correlate of an idling motor area? *Electroencephalography Clinical Neurophysiology*, 98(4), 281-293. doi:10.1016/0013-4694(95)00258-8
- Pope, K. J., Fitzgibbon, S. P., Lewis, T. W., Whitham, E. M., & Willoughby, J. O. (2009). Relation of gamma oscillations in scalp recordings to muscular activity. *Brain Topography*, 22(1), 13-17. doi:10.1007/s10548-009-0081-x
- Raz, N., & Rodrigue, K. M. (2006). Differential aging of the brain: patterns, cognitive correlates and modifiers. *Neuroscience Biobehavioral Reviews*, 30(6), 730-748. doi:10.1016/j.neubiorev.2006.07.001
- Roopun, A. K., Middleton, S. J., Cunningham, M. O., LeBeau, F. E., Bibbig, A., Whittington, M. A., & Traub, R. D. (2006). A beta2-frequency (20–30 Hz) oscillation in nonsynaptic networks of somatosensory cortex. *Proceedings of the National Academy of Sciences*, 103(42), 15646-15650. doi:10.1073/pnas.0607443103
- Rossini, P. M., Rossi, S., Babiloni, C., & Polich, J. (2007). Clinical neurophysiology of aging brain: from normal aging to neurodegeneration. *Progress in Neurobiology*, 83(6), 375-400. doi:10.1016/j.pneurobio.2007.07.010
- Rossiter, H. E., Davis, E. M., Clark, E. V., Boudrias, M.-H., & Ward, N. S. (2014). Beta oscillations reflect changes in motor cortex inhibition in healthy ageing. *NeuroImage*, 91, 360-365. doi:10.1016/j.neuroimage.2014.01.012
- Sakkalis, V. (2011). Review of advanced techniques for the estimation of brain connectivity measured with EEG/MEG. *Computers in Biology and Medicine*, 41(12), 1110-1117. doi:10.1016/j.combiomed.2011.06.020
- Sala-Llonch, R., Junqué, C., Arenaza-Urquijo, E. M., Vidal-Piñero, D., Valls-Pedret, C., Palacios, E. M., . . . Bartrés-Faz, D. (2014). Changes in whole-brain functional

- networks and memory performance in aging. *Neurobiology of Aging*, *35*(10), 2193-2202. doi:10.1016/j.neurobiolaging.2014.04.007
- Sauseng, P., Griesmayr, B., Freunberger, R., & Klimesch, W. (2010). Control mechanisms in working memory: a possible function of EEG theta oscillations. *Neuroscience Biobehavioral Reviews*, *34*(7), 1015-1022. doi:10.1016/j.neubiorev.2009.12.006
- Siegel, M., Donner, T. H., & Engel, A. K. (2012). Spectral fingerprints of large-scale neuronal interactions. *Nature Reviews Neuroscience*, *13*(2), 121. doi:10.1038/nrn3137
- Smit, D. J., Boersma, M., Schnack, H. G., Micheloyannis, S., Boomsma, D. I., Pol, H. E. H., . . . de Geus, E. J. (2012). The brain matures with stronger functional connectivity and decreased randomness of its network. *PloS One*, *7*(5), e36896. doi:10.1371/journal.pone.0036896
- Solesio-Jofre, E., Serbruyns, L., Woolley, D. G., Mantini, D., Beets, I. A., & Swinnen, S. P. (2014). Aging effects on the resting state motor network and interlimb coordination. *Human Brain Mapping*, *35*(8), 3945-3961. doi:10.1002/hbm.22450
- Tomasi, D., & Volkow, N. D. (2012). Aging and functional brain networks. *Molecular Psychiatry*, *17*(5), 549. doi:10.1038/mp.2011.81
- Toussaint, P.-J., Maiz, S., Coynel, D., Messé, A., Perlberg, V., Habert, M. O., & Benali, H. (2011). *Characterization of the default mode functional connectivity in normal aging and Alzheimer's disease: an approach combining entropy-based and graph theoretical measurements*. Paper presented at the Biomedical Imaging: From Nano to Macro, 2011 IEEE International Symposium on.
- van Den Heuvel, M. P., & Hulshoff Pol, H. E. (2010). Exploring the brain network: A review on resting-state fMRI functional connectivity. *European Neuropsychopharmacology*, *20*(8), 519-534. doi:10.1016/j.euroneuro.2010.03.008
- Vysata, O., Kukal, J., Prochazka, A., Pazdera, L., Simko, J., & Valis, M. (2014). Age-related changes in EEG coherence. *Neurologia i neurochirurgia polska*, *48*(1), 35-38. doi:10.1016/j.pjnns.2013.09.001
- Whitham, E. M., Pope, K. J., Fitzgibbon, S. P., Lewis, T., Clark, C. R., Loveless, S., . . . Lillie, P. (2007). Scalp electrical recording during paralysis: quantitative evidence that EEG frequencies above 20 Hz are contaminated by EMG. *Clinical neurophysiology*, *118*(8), 1877-1888. doi:10.1016/j.clinph.2007.04.027
- Wu, J., Quinlan, E. B., Dodakian, L., McKenzie, A., Kathuria, N., Zhou, R. J., . . . Srinivasan, R. (2015). Connectivity measures are robust biomarkers of cortical function and plasticity after stroke. *Brain*, *138*(8), 2359-2369. doi:10.1093/brain/awv156

Wu, J., Srinivasan, R., Kaur, A., & Cramer, S. C. (2014). Resting-state cortical connectivity predicts motor skill acquisition. *NeuroImage*, *91*, 84-90.

doi:10.1016/j.neuroimage.2014.01.026

Wu, T., Zang, Y., Wang, L., Long, X., Hallett, M., Chen, Y., . . . Chan, P. (2007). Aging influence on functional connectivity of the motor network in the resting state.

*Neuroscience letters*, *422*(3), 164-168. doi:10.1016/j.neulet.2007.06.011

## Tables and Figures

**Figure 1.** Grouping electrodes to approximate frontal (F), central (C), temporal (T), parietal (P), and occipital (O) regions.

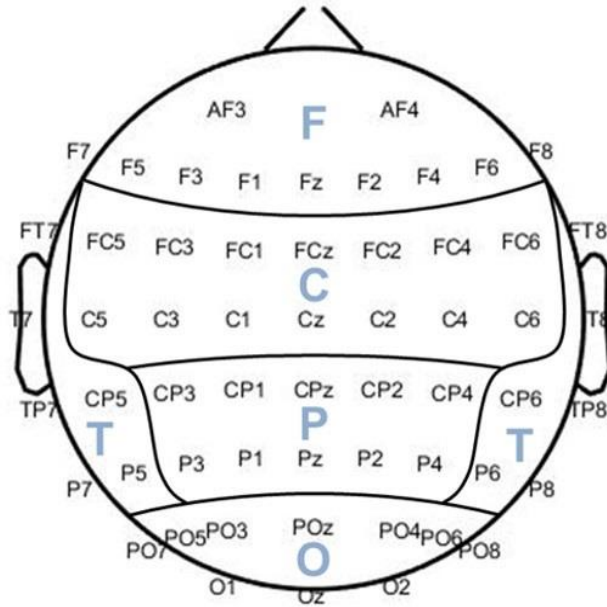
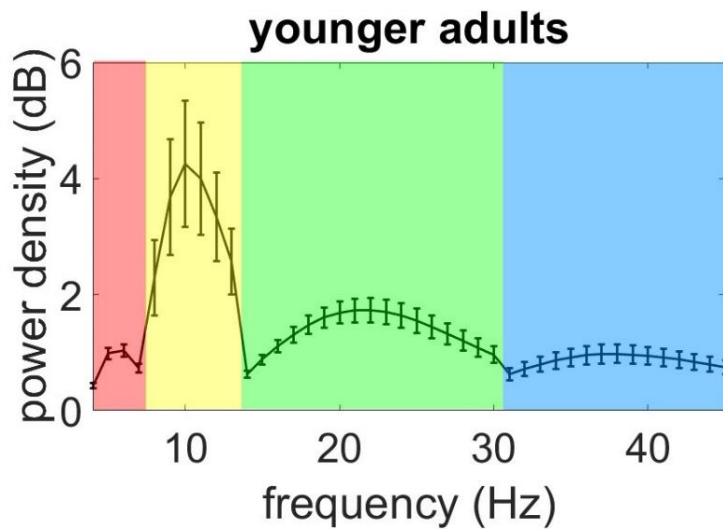
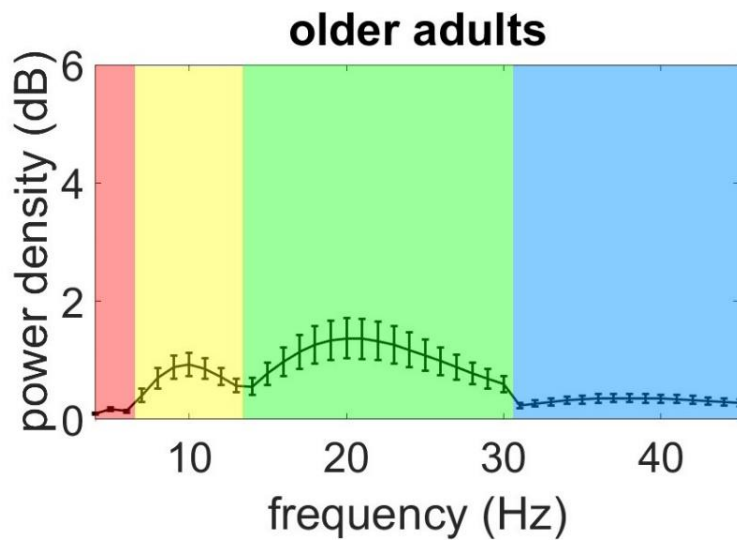


**Figure 2.** Mean Power spectra over all electrodes for (a) younger and (b) older adults. Error bars are SE. Red shade denotes the theta band, yellow shade denotes the alpha band, green shade denotes beta band and blue shade denote the gamma band.



(a)



(b)



**Figure 3.** Illustration of the consensus features with decreased weight with older age (red) and the consensus features with increased weight with older age (blue) in theta, alpha, beta and gamma frequency bands.

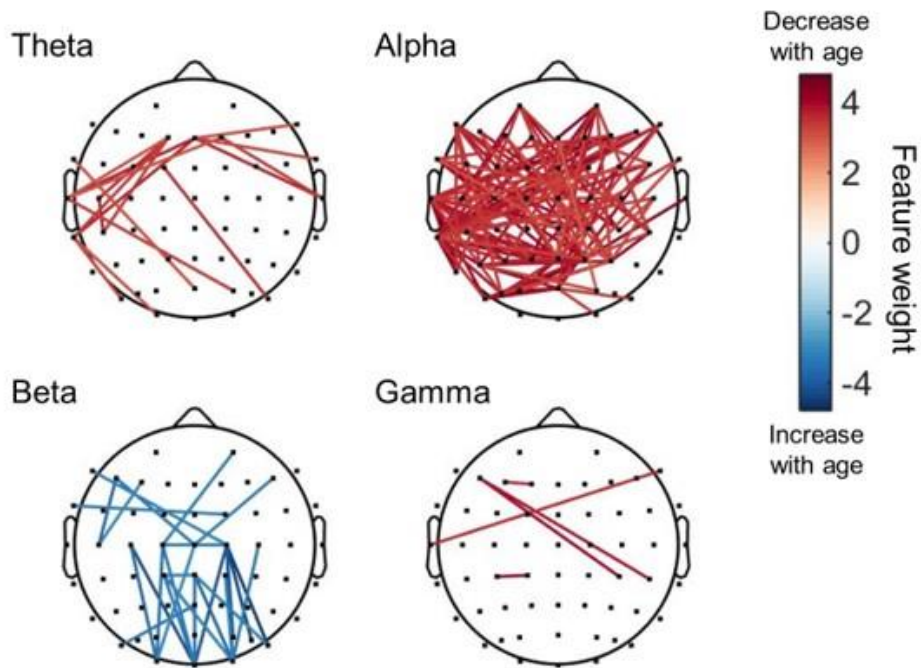


**Figure 4.** Comparison of the contribution of electrodes from each region to the SVM classification (expressed as % of total feature weight). Values are corrected for the total number of electrodes included in each region.

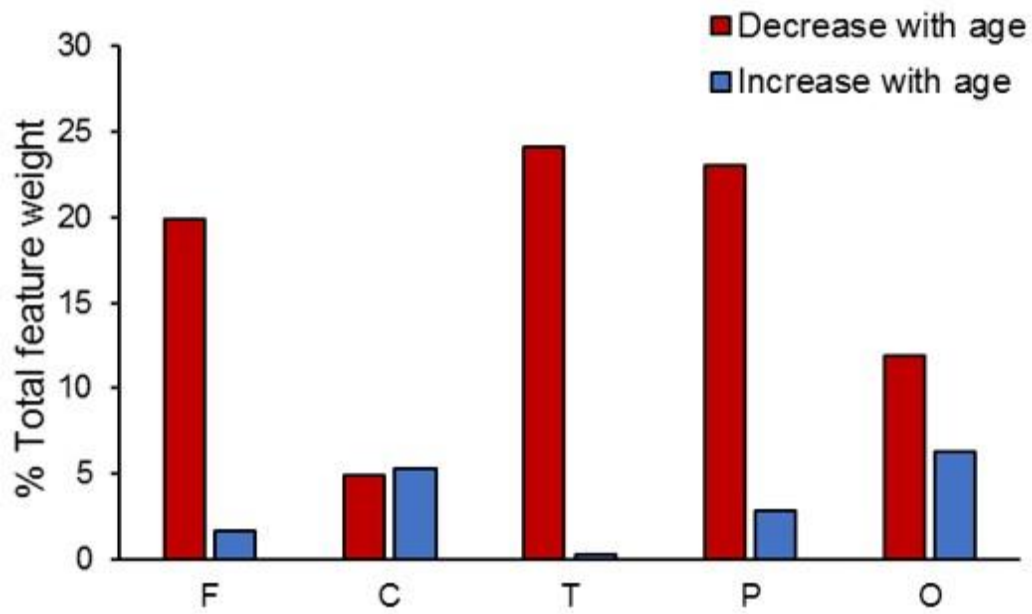


**Figure 5.** Comparison of consensus features with decreased weight with older age to those with increased weight with older age based on electrode-to-electrode distance. Box plots showing the mean (cross), median, interquartile and range of electrode-to-electrode distances for consensus features with decreased weight with older age (red) and those with increased weight with older age (blue). \* $p < 0.01$ .

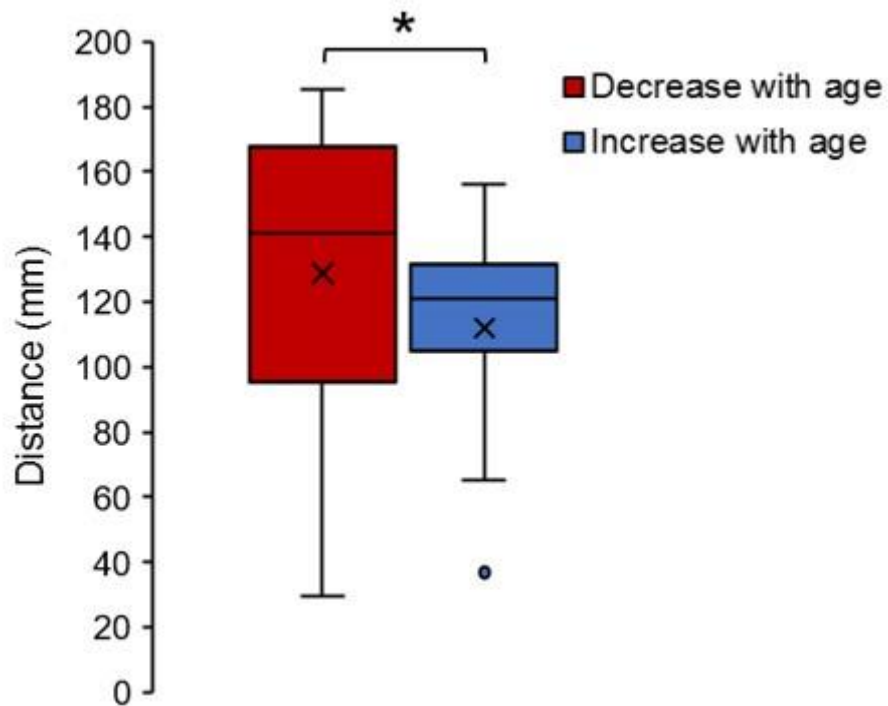


**Table 1.** The accuracy of the different classification methods. SVM: support vector machine, ELM: extreme learning machine, RBF: radial basis function, ROC: receiver operating characteristics.

Method	Accuracy	Area under ROC curve	Young		Old	
			Precision	Recall	Precision	Recall
SVM (RBF kernel)	94%	.97	.89	1.0	1.0	.88
SVM (linear kernel)	80%	.89	.85	.73	.76	.88
K-nearest neighbours	78%	.82	.79	.75	.76	.80
ELM (linear kernel)	70%	.80	.70	.70	.70	.70
ELM (RBF kernel)	80%	.78	.82	.78	.79	.83
ELM (sigmoid kernel)	84%	.84	.87	.80	.81	.88
Least squares linear classifier	68%	.75	.68	.68	.69	.68

## Supplementary material

**Table 2.** Information on consensus features (FDR corrected for multiple comparison,  $q < 0.05$ ). Positive features denote decreased functional connectivity with older age and negative features denote increased functional connectivity with older age.

Frequency	Electrode 1	Electrode 2	Feature weights	P-value
Alpha	T7	F8	4.79	0.0008
Alpha	P2	P5	4.78	0.0008
Beta	C2	O2	-4.74	0.0008
Beta	PO8	C2	-4.71	0.0008
Alpha	PO3	P2	4.61	0.0008
Alpha	TP7	AF4	4.55	0.0008
Alpha	P1	AF4	4.54	0.0008
Alpha	PO5	POz	4.48	0.0008
Beta	PO6	C2	-4.44	0.0008
Alpha	PO5	P2	4.42	0.0008
Beta	Oz	C3	-4.40	0.0008
Alpha	TP7	F8	4.35	0.0008
Alpha	PO3	Pz	4.34	0.0008
Alpha	POz	F4	4.31	0.0008
Alpha	P2	T8	4.31	0.0008
Alpha	PO3	POz	4.31	0.0008
Alpha	TP7	F4	4.30	0.0008
Alpha	TP7	P7	4.30	0.0008
Alpha	P5	POz	4.28	0.0008
Alpha	TP7	P1	4.26	0.0008
Alpha	FT7	Pz	4.25	0.0008
Alpha	FT7	P2	4.24	0.0008
Alpha	TP7	AF3	4.23	0.0008
Alpha	FT7	CP2	4.19	0.0009
Alpha	P7	T7	4.17	0.0010
Alpha	P5	AF4	4.16	0.0010
Alpha	CP4	AF3	4.14	0.0010
Alpha	POz	FC6	4.13	0.0010
Beta	C2	Oz	-4.12	0.0010
Alpha	P4	CP6	4.11	0.0010
Alpha	P5	Pz	4.09	0.0010
Gamma	CP3	CP1	4.07	0.0011
Alpha	P1	F8	4.06	0.0011
Alpha	TP7	Pz	4.06	0.0011
Gamma	CP4	F5	4.02	0.0012
Alpha	TP7	P5	4.02	0.0012
alpha	TP7	Fz	4.00	0.0012

alpha	PO7	T7	4.00	0.0012
alpha	PO7	POz	3.99	0.0012
alpha	CP2	T7	3.97	0.0012
Beta	PO4	C2	-3.97	0.0012
Alpha	P2	P3	3.95	0.0012
Alpha	TP7	F3	3.95	0.0012
Alpha	P2	CP5	3.95	0.0012
Alpha	P5	P4	3.90	0.0014
Alpha	TP7	FC1	3.89	0.0014
Alpha	FC2	POz	3.88	0.0014
Alpha	TP7	FC2	3.88	0.0014
Alpha	TP7	FC6	3.88	0.0014
Alpha	FC4	POz	3.87	0.0014
Alpha	Pz	CP5	3.86	0.0014
Alpha	CP4	F7	3.86	0.0014
Beta	CPz	O2	-3.85	0.0014
Alpha	P2	F7	3.85	0.0014
Alpha	PO7	P2	3.84	0.0014
Alpha	P1	T7	3.83	0.0014
Alpha	AF4	Pz	3.83	0.0014
Alpha	CP4	F5	3.83	0.0014
Alpha	TP7	PO5	3.82	0.0014
Gamma	F5	CP6	3.82	0.0014
Alpha	Pz	T7	3.81	0.0014
Alpha	P2	F3	3.81	0.0014
Alpha	TP7	FC6	3.79	0.0014
Beta	C2	Cz	-3.76	0.0015
Alpha	TP7	FC2	3.76	0.0015
Alpha	FC1	17CP6	3.76	0.0015
Alpha	PO5	Pz	3.75	0.0016
Alpha	Pz	F7	3.75	0.0016
Theta	T7	Fz	3.72	0.0017
Theta	C5	CP5	3.72	0.0017
Beta	C5	F5	-3.71	0.0017
alpha	P3	T7	3.71	0.0017
alpha	FC6	T7	3.71	0.0017
Theta	TP7	Fz	3.70	0.0017
alpha	FC2	T7	3.70	0.0017
alpha	TP7	P3	3.69	0.0017
alpha	P1	CP5	3.68	0.0017
Theta	T8	Fz	3.68	0.0017
Beta	O1	C3	-3.67	0.0017
Alpha	Pz	P3	3.66	0.0018

Alpha	P3	CP5	3.66	0.0018
Alpha	C4	T7	3.63	0.0019
Alpha	P7	F7	3.63	0.0019
Alpha	TP7	C4	3.63	0.0019
Alpha	T7	FC2	3.62	0.0019
Alpha	FC1	P4	3.62	0.0019
Alpha	P5	F7	3.62	0.0019
Alpha	CP2	F7	3.61	0.0019
Alpha	PO7	TP7	3.61	0.0019
Alpha	FT7	F4	3.61	0.0019
Gamma	T7	F8	3.61	0.0019
Beta	C1	O1	-3.60	0.0019
Alpha	AF3	P7	3.60	0.0019
Alpha	CP5	F8	3.59	0.0019
Gamma	FC1	F3	3.59	0.0019
Alpha	AF3	CP6	3.58	0.0019
Alpha	CPz	T7	3.58	0.0019
Alpha	P1	Pz	3.57	0.0020
Alpha	Pz	FC6	3.56	0.0020
Theta	PO8	FC1	3.55	0.0021
Alpha	AF3	P4	3.55	0.0021
Theta	C5	FC1	3.54	0.0021
Alpha	AF4	P3	3.53	0.0022
Alpha	PO7	FC1	3.50	0.0024
Alpha	TP7	FC4	3.49	0.0024
Alpha	PO5	T7	3.49	0.0024
Alpha	AF4	P4	3.48	0.0025
Alpha	C2	T7	3.47	0.0025
Theta	TP7	FC1	3.46	0.0025
Beta	O2	C4	-3.46	0.0025
Alpha	FT8	CPz	3.46	0.0025
Theta	FC2	T8	3.45	0.0025
Alpha	O2	POz	3.45	0.0025
Theta	PO4	T7	3.45	0.0025
Beta	C1	Oz	-3.45	0.0025
Beta	Oz	CP1	-3.43	0.0027
Alpha	FC2	FC6	3.42	0.0027
Beta	PO7	Pz	-3.42	0.0027
Alpha	PO5	P4	3.42	0.0027
Alpha	PO8	POz	3.42	0.0027
Alpha	P1	C5	3.41	0.0027
Alpha	AF4	CP6	3.41	0.0027
Theta	FC1	CP5	3.41	0.0027

Beta	CPz	Oz	-3.40	0.0027
Alpha	TP7	C6	3.38	0.0028
Alpha	Pz	F8	3.37	0.0029
Alpha	PO5	F7	3.37	0.0030
Alpha	P2	AF3	3.35	0.0031
Beta	F5	Cz	-3.35	0.0031
Alpha	PO3	P4	3.34	0.0031
Alpha	P2	CP6	3.33	0.0032
Theta	PO7	TP7	3.33	0.0032
Alpha	CP4	C6	3.32	0.0032
Alpha	P4	F3	3.32	0.0033
Alpha	F5	Pz	3.31	0.0033
Beta	O2	CP1	-3.30	0.0034
Alpha	FC2	Pz	3.30	0.0034
Beta	CPz	CP1	-3.29	0.0035
Theta	FT8	Fz	3.28	0.0035
Beta	C2	F7	-3.28	0.0035
Beta	PO8	CPz	-3.27	0.0036
Beta	O2	CP2	-3.26	0.0037
Beta	C1	AF4	-3.25	0.0037
Alpha	Pz	Fz	3.25	0.0037
Alpha	PO4	P5	3.24	0.0038
Beta	FT7	FC2	-3.24	0.0038
Alpha	C6	P4	3.24	0.0038
Alpha	FT8	P2	3.23	0.0039
Alpha	FT7	C4	3.22	0.0040
Alpha	C5	FC6	3.21	0.0041
Alpha	TP7	P2	3.21	0.0041
Beta	C2	C1	-3.20	0.0041
Beta	FC6	Cz	-3.20	0.0042
Beta	C5	F3	-3.19	0.0043
Theta	F8	Fz	3.18	0.0043
Beta	O1	Cz	-3.17	0.0044
Alpha	FT7	P4	3.17	0.0044
Theta	TP7	O1	3.15	0.0046
Theta	FC1	T7	3.13	0.0050
Theta	FC2	T7	3.11	0.0052
Theta	FT7	POz	3.05	0.0061
Alpha	PO4	Fz	3.02	0.0068